

of these two states. The second point concerns a possibly nonlinear PtCO. We find both the SCF  $^1\Sigma^+$  and  $^3\Sigma^+$  states to be strongly linear. Clark et al.<sup>26</sup> found the  $^3\Delta$  state in NiCO to be weakly bent, and the same behavior is expected also for  $^3\Delta$  in PtCO. Therefore, bending PtCO is not expected to change the ordering of electronic states found for the linear geometric configuration.

**Acknowledgment.** We wish to thank Dr. S. T. Elbert for supplying us with his latest version of ALIS. This work has been supported by the Israel Commission for Basic Research, Jerusalem, Israel. We acknowledge very useful comments by the reviewers.

Registry No. PtCO, 49819-49-0.

## Electronic Structure of Alkylated Imidazoles and Electronic Spectra of Tetrakis(imidazole)copper(II) Complexes. Molecular Structure of Tetrakis(1,4,5-trimethylimidazole)copper(II) Diperchlorate

Ernest Bernarducci, Parimal K. Bharadwaj, Karsten Krogh-Jespersen,\* Joseph A. Potenza,\* and Harvey J. Schugar\*

Contribution from the Department of Chemistry, Rutgers, The State University of New Jersey, New Brunswick, New Jersey 08903. Received September 7, 1982

**Abstract:** The synthesis, crystal structure, electronic spectra, and ESR spectra are reported for the title complex (1). This complex crystallized as orange-brown plates in the orthorhombic space group *Pccn* with  $a = 13.65$  (1) Å,  $b = 13.90$  (1) Å, and  $c = 17.54$  (1) Å,  $d_{\text{obsd}} = 1.40$  (1) g/cm<sup>3</sup>,  $d_{\text{calcd}} = 1.403$  g/cm<sup>3</sup>, and  $Z = 4$ . Least-squares refinement of 1346 reflections having  $F^2 \geq 3\sigma$  gave a conventional *R* factor of 0.063 and  $R_{\text{wF}} = 0.060$ . The structure consists of discrete tetrakis(1,4,5-trimethylimidazole)copper(II) cations with point symmetry  $\bar{1}$  whose planar  $\text{CuN}_4$  units exhibit Cu-N distances of 2.004 (7) and 1.995 (7) Å and N-Cu-N angles of 89.5 (3) and 90.5 (3)°. Dihedral angles between the imidazole and  $\text{CuN}_4$  planes are 75.7 and 75.5°. Energies of the molecular orbitals and electronically excited states of imidazole and of several methylated imidazoles have been calculated by an INDO/S method. The observed ligand  $\pi \rightarrow \pi^*$  and  $n, \pi_1, \pi_2(\text{ligand}) \rightarrow \text{Cu(II)}$  ligand to metal charge-transfer (LMCT) absorptions of the title complex and other Cu(II)-imidazole complexes are discussed and compared. Preliminary LMCT spectra are presented for the yellow diamagnetic tetrakis(1,2-dimethylimidazole)nickel(II) diperchlorate complex and its Cu(II) analogue. An experimental justification for assigning the charge-transfer absorptions as LMCT instead of MLCT is presented.

The presence of Cu(II)-imidazole bonding in proteins has been demonstrated crystallographically for plastocyanin,<sup>1</sup> azurin,<sup>2</sup> and superoxide dismutase<sup>3</sup> and has been inferred for stellacyanin,<sup>4</sup> serum albumin,<sup>5</sup> galactose oxidase,<sup>6</sup> cytochrome *c* oxidase,<sup>7</sup> ceruloplasmin,<sup>8</sup> hemocyanins,<sup>9</sup> and tyrosinases.<sup>10</sup> The wide biochemical scope of Cu(II)-imidazole bonding has prompted numerous spectroscopic studies of low molecular weight Cu(II) chromophores including ligation from imidazoles, histidine, histamine, and histidine-containing peptides. Tetragonal Cu(II) chromophores of these types exhibit four or five absorption maxima in the 29 000-45 000-cm<sup>-1</sup> spectral region, including a weak near-UV band or shoulder ( $\epsilon \sim 300$ ) thought to arise from  $\pi$ -

(imidazole)  $\rightarrow$  Cu(II) ligand to metal charge-transfer (LMCT).<sup>9,11,12</sup> We have chosen to elaborate the nature of imidazole  $\rightarrow$  Cu(II) LMCT absorptions exhibited by well-defined model Cu(II) complexes to help facilitate the assignment of corresponding absorptions in the spectra of various Cu(II) protein chromophores. These studies have yielded several useful results.<sup>13,14</sup> First, Cu(II)-imidazole chromophores exhibit three types of LMCT absorptions that originate from the  $sp^2$  nitrogen lone pair ( $n$ ) and from two  $\pi$ -symmetry ring orbitals, one (HOMO,  $\pi_1$ ) with mostly carbon character and the other ( $\pi_2$ ) with substantial nitrogen character. Tetragonal Cu(II)-imidazole complexes exhibit overlapping  $n(\text{imidazole}) \rightarrow \text{Cu(II)}$  LMCT and ligand  $\pi \rightarrow \pi^*$  absorptions at  $\sim 45$  000 cm<sup>-1</sup>; the  $\pi_2(\text{imidazole}) \rightarrow \text{Cu(II)}$  and  $\pi_1(\text{imidazole}) \rightarrow \text{Cu(II)}$  LMCT absorptions occur at approximately 35 000 and 30 000 cm<sup>-1</sup>, respectively. Corresponding  $\pi(\text{imidazole}) \rightarrow \text{Cu(II)}$  LMCT absorptions have been noted in the UV spectra of native and two types of Cu(II)-doped superoxide dismutase.<sup>15</sup> Second, owing to the small ligand fields<sup>16</sup>

(1) Coleman, P. M.; Freeman, H. C.; Guss, J. M.; Murata, M.; Norris, V. A.; Ramshaw, J. A. M.; Venkatappa, M. P. *Nature (London)* **1980**, *272*, 319-24.

(2) Adman, E. T.; Stienkamp, R. E.; Sieker, L. C.; Jensen, L. H. *J. Mol. Biol.* **1978**, *123*, 35-47.

(3) Richardson, J. E.; Thomas, K. A.; Rubin, B. H.; Richardson, D. C. *Proc. Natl. Acad. Sci. U.S.A.* **1975**, *72*, 1349-52.

(4) Ulrich, E. L.; Markley, J. L. *Coord. Chem. Rev.* **1978**, *27*, 109-40.

(5) Bradshaw, R. A.; Shearer, W. T.; Gurd, F. R. N. *J. Biol. Chem.* **1968**, *243*, 3817-25.

(6) Bereman, R. D.; Kosman, D. J. *J. Am. Chem. Soc.* **1977**, *99*, 7322-25.

(7) Palmer, G.; Babcock, G. T.; Vickery, L. E. *Proc. Natl. Acad. Sci. U.S.A.* **1976**, *73*, 2206-10.

(8) Fee, J. A. *Struct. Bonding (Berlin)* **1975**, *23*, 1-60.

(9) Freedman, T. B.; Loehr, J. S.; Loehr, T. M. *J. Am. Chem. Soc.* **1976**, *98*, 2809-15.

(10) Himmelwright, R. S.; Eickman, N. C.; LuBien, C. D.; Lerch, K.; Solomon, E. I. *J. Am. Chem. Soc.* **1980**, *102*, 7339-44.

(11) Bryce, G. F.; Gurd, F. R. N. *J. Biol. Chem.* **1966**, *241*, 122-29.

(12) Amundsen, A. R.; Whelan, J.; Bosnich, B. *J. Am. Chem. Soc.* **1977**, *99*, 6730-39.

(13) Fawcett, T. G.; Bernarducci, E.; Krogh-Jespersen, K.; Schugar, H. J. *J. Am. Chem. Soc.* **1980**, *102*, 2598-2604.

(14) Bernarducci, E.; Schwindinger, W. F.; Hughey, J. L., IV; Krogh-Jespersen, K.; Schugar, H. J. *J. Am. Chem. Soc.* **1981**, *103*, 1686-91.

(15) Pantoliano, M. W.; Valentine, J. S.; Nafie, L. A. *J. Am. Chem. Soc.* **1982**, *104*, 6310-17.

(16) Solomon, E. I.; Hare, J. W.; Dooley, D. M.; Dawson, J. H.; Stephens, P. J.; Gray, H. B. *J. Am. Chem. Soc.* **1980**, *102*, 168-78.

experienced by the type 1 blue copper chromophores, the LMCT absorptions of such chromophores will be red-shifted relative to those exhibited by typical tetragonal and trigonal-bipyramidal Cu(II) chromophores. We have suggested that this red-shift amounts to 10 000–12 000  $\text{cm}^{-1}$ ; consequently,  $\pi(\text{imidazole}) \rightarrow \text{Cu(II)}$  LMCT absorptions are expected in the visible–near-UV spectra of type 1 Cu(II) chromophores.<sup>16,17</sup> Third, we have suggested that facile rotation about the Cu(II)–N(imidazole) bonds of the solution complex led to a wide range of  $\pi(\text{ligand})\text{--Cu}(d_{x^2-y^2})$  overlaps and was responsible for the weak ( $\epsilon \sim 350$ ) unresolved  $\pi_1, \pi_2(\text{imidazole}) \rightarrow \text{Cu(II)}$  LMCT absorption of aqueous  $\text{Cu}(\text{im})_4^{2+}$  (im = imidazole). Since the ease of rotation about a metal–N(imidazole) bond is sensitive to steric effects,<sup>18</sup> we decided to investigate the solution spectra of Cu(II) complexed with bulky imidazole ligands. Solution spectra of tetrakis Cu(II) complexes of various 4,5-dialkylated imidazoles exhibit well-resolved and prominent ( $\epsilon \sim 2000$ )  $\pi_1$ - and  $\pi_2(\text{imidazole}) \rightarrow \text{Cu(II)}$  LMCT absorptions at  $\sim 33\,000$  and  $\sim 29\,000$   $\text{cm}^{-1}$ , respectively. Unfortunately, we were not able to prepare these complexes in crystalline form. However, the tetrakis Cu(II) complex of 1,4,5-trimethylimidazole (1,4,5-tmi) also exhibits well-resolved solution spectra and could be crystallized as the diperchlorate salt.

We report here the molecular structure and electronic spectra of the title complex (1). Further, we discuss the effect of ring alkylation on the calculated (INDO/S) energies of the upper occupied ligand orbitals and the observed LMCT spectra. We also present preliminary electronic spectra of the Ni(1,2-dmi)<sub>4</sub>·2ClO<sub>4</sub> complex (1,2-dmi = 1,2-dimethylimidazole) and its Cu(II) analogue and demonstrate that the charge-transfer absorptions of various M(II)–imidazole chromophores (M = Cu(II), Ni(II)) are LMCT, not MLCT, in nature.

### Experimental Section

**Preparation of 4,5-Dimethylimidazole.** Acetone was converted to 4,5-dimethylimidazole by following a published procedure.<sup>19</sup> A mixture containing 200 mL of formamide and 36 g of 85% aqueous acetone (Aldrich Chemical Co.) was refluxed for 5 h; the reaction temperature gradually rose to 443 K and then remained constant. After removal of the excess formamide by vacuum distillation, the product was obtained in 63% yield as a fraction that boiled at 388–392 K ( $\sim 1$  mmHg) (lit.<sup>19</sup> bp 438–448 K (10 mmHg)). An occasional application of a heat lamp was required to keep the product from solidifying in the air-cooled condenser. The waxy product was hygroscopic and used without further purification; <sup>1</sup>H NMR (CDCl<sub>3</sub>, 60 MHz)  $\delta$  2.2 (s, 6H, CH<sub>3</sub>), 7.7 (s, 1H, Ar H), 9.0 (s, 1H, NH).

**Preparation of 1,4,5-Trimethylimidazole.** CH<sub>3</sub>I (15 mL) was added dropwise to a mixture containing 250 mL of anhydrous NH<sub>3</sub>(l), 5.4 g of Na, a small crystal of ferric nitrate, and 18.9 g of 4,5-dimethylimidazole.<sup>20</sup> Following removal of the NH<sub>3</sub> by evaporation, water was added to the resulting solid, and the product imidazole was extracted with CH<sub>2</sub>Cl<sub>2</sub>. The solvent was removed by rotoevaporation. Vacuum distillation yielded the product as a fraction that boiled at 338–346 K ( $\sim 1$  mmHg). The waxy hygroscopic product was further purified by sublimation (333 K ( $\sim 1$  mmHg)) and finally obtained in 33% yield; <sup>1</sup>H NMR (CDCl<sub>3</sub>, 60 MHz)  $\delta$  2.17 (s, 6H, CH<sub>3</sub>), 3.5 (s, 3H, CH<sub>3</sub>), 7.3 (s, 1H, Ar H).

**Preparation of Cu(1,4,5-tmi)<sub>4</sub>·2ClO<sub>4</sub> (1).** This complex precipitated immediately as an orange solid from a solution of 0.84 g of Cu(ClO<sub>4</sub>)<sub>2</sub>·6H<sub>2</sub>O (2.3 mmol) and 1.0 g of ligand (9.1 mmol) in 20 mL of dry CH<sub>3</sub>OH. The complex was recrystallized from CH<sub>3</sub>OH. Slow evaporation of the resulting blue-green solutions yielded well-formed orange-brown plates that were suitable for X-ray diffraction studies. The crystals were stable in air and did not exhibit sensitivity toward shock. We did not elect to heat these crystals for melting point or other measurements. Anal. Calcd for CuC<sub>24</sub>H<sub>40</sub>N<sub>8</sub>Cl<sub>2</sub>O<sub>8</sub>: Cu, 9.03; C, 41.01; H, 5.74; N, 15.94. Found: Cu, 8.99; C, 40.91; H, 5.73; N, 15.87.

**Preparation of Ni(1,2-dmi)<sub>4</sub>·2ClO<sub>4</sub>.** This complex, previously prepared by Reedijk,<sup>21</sup> crystallized as well-formed yellow plates when green-yellow

solutions containing 0.46 g (1.25 mmol) of Ni(ClO<sub>4</sub>)<sub>2</sub>·6H<sub>2</sub>O and 0.52 g (5.4 mmol) of 1,2-dimethylimidazole (Aldrich Chemical Co.) in a mixture of 30 mL of acetone and 5 mL of methanol were allowed to evaporate at room temperature. The crystals were stable in air and did not exhibit sensitivity toward shock. We did not elect to heat these crystals to determine their melting point (lit.<sup>21</sup> mp 553–557 K). The crystals were diamagnetic at 298 K, and their density was determined (floatation, cyclohexane/dibromoethane) to be 1.45 (1) g/cm<sup>3</sup>. The concentration of Ni(II) in the neat complex is 2.26 M. Anal. Calcd for NiC<sub>20</sub>H<sub>32</sub>N<sub>8</sub>Cl<sub>2</sub>O<sub>8</sub>: Ni, 9.15; C, 37.39; H, 5.03; N, 17.46. Found: Ni, 8.83; C, 36.72; H, 4.94; N, 17.26.

**Preparation of Cu(1,2-dmi)<sub>4</sub>·2ClO<sub>4</sub>.** This complex has been prepared previously by Reedijk.<sup>21</sup> A solution consisting of 0.370 g of Cu(ClO<sub>4</sub>)<sub>2</sub>·6H<sub>2</sub>O (1.0 mmol) in 10 mL of dry methanol was added to a solution of 0.336 g (4.0 mmol) of freshly distilled ligand also in 10 mL of dry methanol. Slow evaporation in air yielded the complex as blue-purple prisms. The crystals were stable in air. Anal. Calcd for CuC<sub>20</sub>H<sub>32</sub>N<sub>8</sub>Cl<sub>2</sub>O<sub>8</sub>: Cu, 9.82; C, 37.13; H, 4.98; N, 17.32. Found: Cu, 9.62; C, 36.72; H, 4.78; N, 17.16.

**Preparation of Cu(im)<sub>4</sub>·2NO<sub>3</sub>.** This complex crystallizes as deep blue-purple prisms from ethanolic solutions containing Cu(NO<sub>3</sub>)<sub>2</sub>·6H<sub>2</sub>O and imidazole in a 1:4 ratio. An examination of Weissenberg photographs verified that the crystals in fact were the orthorhombic Cu(im)<sub>4</sub>·2NO<sub>3</sub> phase that has been characterized structurally by other workers.<sup>22</sup>

**X-ray Diffraction Studies.** A crystal of the title complex approximately 0.44 × 0.28 × 0.30 mm was glued to a glass fiber. Preliminary Weissenberg photographs indicated an orthorhombic system. Unit cell constants ( $a = 13.65$  (1),  $b = 13.90$  (1),  $c = 17.54$  (1) Å) were determined by a least-squares fit of ten moderately intense high-angle reflections accurately centered on an Enraf-Nonius CAD-III diffractometer using graphite-monochromated Mo K $\alpha$  radiation ( $\lambda = 0.71069$  Å). Diffractometer examination of the reciprocal lattice showed the space group to be *Pccn* from the following systematic absences:  $0kl, l = 2n + 1; h0l, l = 2n + 1; hk0, h + k = 2n + 1$ . With  $Z = 4$ , the observed (1.40 (1) g/cm<sup>3</sup>) and calculated (1.403 g/cm<sup>3</sup>) densities agreed well. Intensity data ( $\theta$ – $2\theta$  scan,  $4 \leq 2\theta \leq 45^\circ$ ) were collected at 298 (1) K and corrected for decay, Lp effects, and absorption ( $1.26 \leq A \leq 1.46$ ) as described previously.<sup>23</sup> Two standard reflections, measured at 30 reflection intervals, remained constant to  $\pm 5\%$  throughout the data collection period. Of the 2502 unique reflections measured, 1346 with  $F^2 \geq 3\sigma(F^2)$  (counting statistics) were used in the structure solution and refinement. The structure was solved by direct methods<sup>24</sup> and refined by full-matrix least-squares techniques. Neutral-atom scattering factors<sup>25</sup> were used, and anomalous dispersion corrections<sup>26</sup> were applied to the Cu and Cl atoms. An E map, calculated by using 350 phases from the starting set with the highest combined figure of merit, revealed all the non-hydrogen atoms. Several cycles of isotropic unit weight refinement followed by several cycles of anisotropic refinement led to convergence with  $R_F = \sum ||F_o| - |F_c|| / \sum |F_o| = 0.091$ .

Hydrogen atoms were added to the model at calculated positions with N–H and C–H bond lengths taken to be 0.87 and 0.95 Å, respectively.<sup>27</sup> A planar geometry was assumed for the aromatic C atoms, while methyl C atoms were assumed to be tetrahedral. Methyl H atoms were located by rotating at  $5^\circ$  intervals the idealized tetrahedral positions and computing the electron density at these positions. The orientation with the highest combined electron density was used. H atoms were assigned temperature factors according to  $B_H = B_N + 1$ , where  $N$  is the atom bonded to H. Hydrogen atom parameters were not refined. Additional refinement, using anisotropic thermal parameters for all non-hydrogen atoms, reduced  $R_F$  to 0.063 and  $R_{wF} = (\sum w(|F_o| - |F_c|)^2 / \sum wF_o^2)^{1/2}$  to 0.060. For the final cycle, all parameter changes were within  $0.04\sigma$ , where  $\sigma$  is the estimated standard deviation obtained from the inverse matrix. A final difference map showed a general background of ap-

(22) Eilbeck, W. J.; Holmes, F.; Underhill, A. E. *J. Chem. Soc. A* **1967**, 757–61. McFadden, D. L.; McPhail, A. T.; Garner, C. D.; Mabbs, F. E. *J. Chem. Soc., Dalton Trans.* **1976**, 47–52.

(23) Hughey, J. L., IV; Fawcett, T. G.; Rudich, S. M.; Lalancette, R. A.; Potenza, J. A.; Schugar, H. J. *J. Am. Chem. Soc.* **1979**, *101*, 2617–23.

(24) In addition to local programs for the IBM 370/168 computer, local modifications of the following programs were employed: Coppens' ABSORB program; Zalkin's FORDP Fourier program; Johnson's ORTEP II thermal ellipsoid plotting program; Busing, Martin, and Levy's ORFFE error function program; Main, Lessinger, Declercq, Woolfson, and Germain's MULTAN 78 program for the automatic solution of crystal structures; the FLINUS least-squares program obtained from Brookhaven National Laboratories.

(25) Cromer, D. T.; Waber, J. T. *Acta Crystallogr.* **1965**, *18*, 104–9.

(26) "International Tables for X-ray Crystallography"; Kynoch Press: Birmingham, England, 1962; Vol. III, pp 201–13.

(27) Churchill, M. R. *Inorg. Chem.* **1973**, *12*, 1213–4.

(17) Penfield, K. W.; Gay, R. R.; Himmelwright, R. S.; Eickman, N. C.; Norris, V. A.; Freeman, H. C.; Solomon, E. I. *J. Am. Chem. Soc.* **1981**, *103*, 4382–88.

(18) Freeman, H. B. In "Inorganic Biochemistry"; Eichorn, G., Ed.; American Elsevier: New York, 1973; Vol. 1, Chapter 3.

(19) Bredereck, H.; Thellig, G. *Chem. Ber.* **1953**, *86*, 88–93.

(20) Roe, A. M. *J. Chem. Soc.* **1963**, 2195–2200.

(21) Reedijk, J. *Recl. Trav. Chim. Pays-Bas* **1972**, *91*, 1373–82.

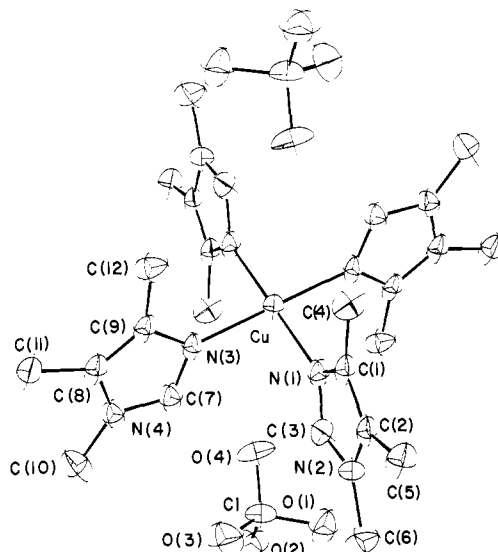


**Figure 1.** ORTEP view of the title complex **1** showing the atom numbering scheme.

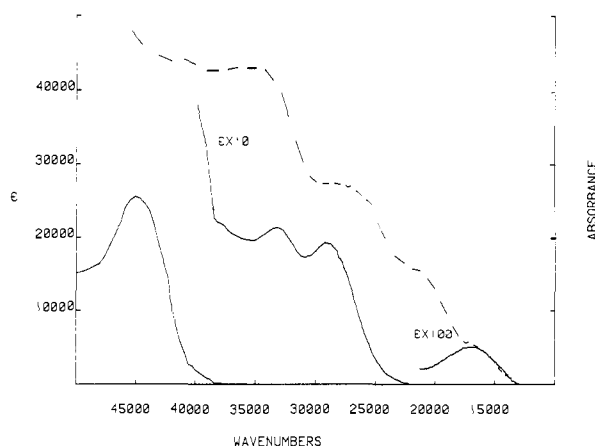


**Figure 2.** Electronic spectra of **1** at 80 K as a mineral oil mull (---) and at 298 K as a 3.5 mM solution in  $\text{CH}_3\text{OH}$  (—). Solution spectra of the free ligand at 298 K are indicated by the dotted line.

proximately  $\pm 0.3 \text{ e}/\text{\AA}^3$  and revealed no unusual features. Final atomic parameters are listed in Table I while a view of the complex is given in Figure 1. Lists of observed and calculated structure factors, anisotropic thermal parameters, calculated H atom parameters, and a stereoscopic view of the unit cell contents are available.<sup>28</sup>

**Physical Measurements.** Electronic spectra were recorded using a Cary Model 17 R1 spectrophotometer. Presentation of the data on linear energy scales (Figure 3) was facilitated by a Tektronix Model 4052 computer/plotter system. ESR spectra were measured by using a Varian Model E-12 spectrometer calibrated with a Hewlett-Packard Model 5245 L frequency counter and a DPPH crystal ( $g = 2.0036$ ). The diamagnetism<sup>21</sup> of  $\text{Ni}(\text{1,2-dmi})_4\cdot 2\text{ClO}_4$  at 298 K was established by using a Faraday balance calibrated with  $\text{HgCo}(\text{SCN})_4$ .

**Calculational Details.** Molecular orbital calculations on imidazoles methylated in various ways have been performed by using an INDO/S method.<sup>29</sup> Values for the one-center, two-electron integrals  $\gamma_{AA}$  were taken from Del Bene and Jaffé.<sup>30</sup> Two-center, two-electron integrals  $\gamma_{AB}$  were evaluated by the interpolation formula proposed by Mataga and Nishimoto.<sup>31</sup> The atomic parameters  $\beta_A^\circ$  are those of Ellis et al.<sup>32</sup> with  $\pi$ -screening constants  $K_{CC} = 0.570$  and  $K_{CN} = K_{NN} = 0.585$ . Bond distances and angles were based upon the ligand geometries determined

**Table I.** Fractional Atomic Coordinates and Equivalent Isotropic Temperature Factors for **1**<sup>a</sup>

	x	y	z	$B_{\text{eq}}, \text{\AA}^2$ <sup>b</sup>
Cu	0.500	0.0	0.0	4.08 (3)
Cl	0.4963 (3)	0.0684 (2)	0.29102 (14)	6.55 (7)
O(1)	0.5979 (6)	0.1031 (6)	0.2853 (5)	10.3 (3)
O(2)	0.4868 (7)	0.0318 (6)	0.3667 (4)	9.3 (2)
O(3)	0.4330 (7)	0.1460 (6)	0.2758 (6)	10.7 (3)
O(4)	0.4893 (7)	-0.0043 (6)	0.2353 (4)	8.3 (2)
N(1)	0.5635 (5)	0.1256 (5)	0.0263 (5)	5.0 (2)
N(2)	0.6094 (5)	0.2498 (6)	0.0944 (5)	5.4 (2)
C(1)	0.5917 (6)	0.1979 (6)	-0.0226 (6)	4.9 (3)
C(2)	0.6208 (6)	0.2740 (6)	0.0184 (6)	5.0 (3)
C(3)	0.5743 (7)	0.1602 (7)	0.0963 (7)	5.9 (3)
C(4)	0.5912 (8)	0.1853 (7)	-0.1077 (6)	6.8 (3)
C(5)	0.6569 (7)	0.3734 (6)	-0.0034 (7)	6.5 (3)
C(6)	0.6275 (9)	0.3083 (8)	0.1616 (8)	8.8 (4)
N(3)	0.3702 (6)	0.0554 (5)	0.0283 (5)	4.6 (2)
N(4)	0.2495 (6)	0.1081 (5)	0.1008 (5)	5.4 (2)
C(7)	0.3396 (7)	0.0676 (7)	0.0994 (7)	5.5 (3)
C(8)	0.2212 (7)	0.1204 (6)	0.0260 (7)	5.6 (3)
C(9)	0.2960 (7)	0.0884 (6)	-0.0167 (6)	5.1 (3)
C(10)	0.1923 (9)	0.1292 (9)	0.1679 (7)	8.5 (4)
C(11)	0.1227 (7)	0.1604 (7)	0.0059 (8)	7.5 (4)
C(12)	0.3051 (8)	0.0864 (8)	-0.1025 (6)	7.1 (3)

<sup>a</sup> Estimated standard deviations are given in parentheses. <sup>b</sup>  $B_{\text{eq}} = (8\pi^2/3)(U_{11}a^*a^2 + U_{12}a^*b^*ab \cos \gamma + \dots)$ .

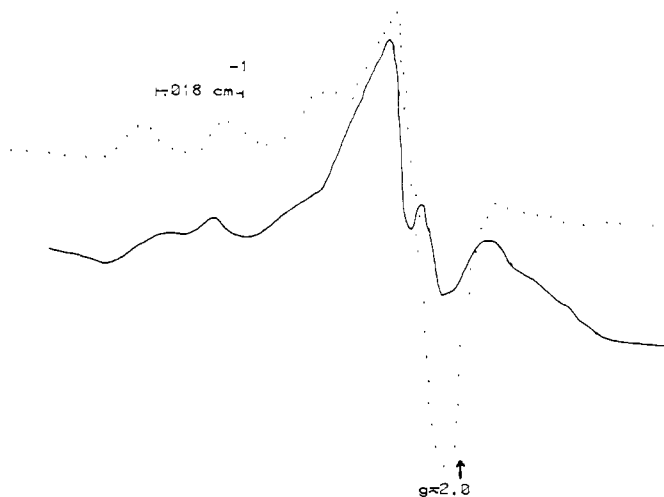


**Figure 3.** ESR spectra of **1** ( $\sim 3.5 \text{ mM}$ ) in  $\text{CH}_3\text{OH}$  at  $\sim 298 \text{ K}$  (—) and at  $\sim 223 \text{ K}$  (···).

crystallographically in this work and other published studies.<sup>33</sup> The electronically excited states were calculated in the singly excited configuration interaction approximation with all configurations of the  $(n, \pi^*)$ - and  $(\pi, \pi^*)$ -type included; oscillator strengths were determined with the dipole length operator. The calculated orbital and transition energies are relatively insensitive to small changes in the atomic parameters or molecular geometries employed.

## Results and Discussion

**Description of the Structure.** The structure of **1** consists of discrete  $\text{Cu}(\text{1,4,5-tmi})_4^{2+}$  cations with point symmetry  $\bar{1}$  separated by perchlorate anions. The equatorial  $\text{N}_4$  coordination of the Cu atom is planar (crystallographically required). Apical ligation is not present; all Cu-O(perchlorate) distances are greater than 4 Å. Structural parameters are presented in Tables II and III. Bond distances (2.004 (7), 1.995 (7) Å) and angles (89.5 (3), 90.5 (3)°) within the  $\text{CuN}_4$  unit are typical for tetrakis(imidazole)-copper(II) complexes.<sup>22,33</sup> There are two crystallographically different 1,4,5-trimethylimidazole ligands present, although corresponding structural parameters of both are the same within experimental error. Bond distances and angles within the five-

(28) Supplementary material.

(29) Krogh-Jespersen, K.; Ratner, M. A. *Theor. Chim. Acta* **1978**, *47*, 283-96.

(30) Del Bene, J.; Jaffé, H. H. *J. Chem. Phys.* **1968**, *48*, 1807-13.

(31) Mataga, N.; Nishimoto, K. *Z. Phys. Chem.* **1957**, *13*, 140-57.

(32) Ellis, R. L.; Kuehnlenz, G.; Jaffé, H. H. *Theor. Chim. Acta* **1972**, *26*, 131-40.

(33) Fransson, G.; Lundberg, B. K. S. *Acta Chem. Scand.* **1972**, *26*, 3969-76.

Table II. Selected Bond Distances (Å) and Angles (deg) in 1

Coordination Sphere			
Cu-N(1)	2.004 (7)	Cu-N(3)	1.995 (7)
Imidazole Rings			
N(1)-C(1)	1.376 (11)	N(3)-C(9)	1.364 (11)
C(1)-C(2)	1.340 (12)	C(9)-C(8)	1.342 (12)
C(2)-N(2)	1.384 (11)	C(8)-N(4)	1.378 (12)
N(2)-C(3)	1.336 (11)	N(4)-C(7)	1.354 (11)
C(3)-N(1)	1.326 (12)	C(7)-N(3)	1.326 (12)
C(1)-C(4)	1.504 (14)	C(9)-C(12)	1.511 (14)
C(2)-C(5)	1.516 (12)	C(8)-C(11)	1.498 (12)
N(2)-C(6)	1.454 (13)	N(4)-C(10)	1.443 (12)
Perchlorate			
Cl-O(1)	1.473 (8)	Cl-O(3)	1.408 (8)
Cl-O(2)	1.428 (7)	Cl-O(4)	1.410 (7)
Coordination Sphere			
N(1)-Cu-N(3)	89.5 (3)	N(1)-Cu-N(3')	90.5 (3)
Cu-N(1)-C(1)	127.8 (7)	Cu-N(3)-C(9)	130.2 (7)
Cu-N(1)-C(3)	125.2 (7)	Cu-N(3)-C(7)	124.3 (6)
Imidazole Rings			
C(1)-N(1)-C(3)	106.4 (7)	C(9)-N(3)-C(7)	105.5 (8)
C(2)-C(1)-N(1)	109.0 (9)	C(8)-C(9)-N(3)	110.7 (9)
N(2)-C(2)-C(1)	106.9 (8)	N(4)-C(8)-C(9)	106.1 (8)
C(3)-N(2)-C(2)	106.9 (8)	C(7)-N(4)-C(8)	106.8 (9)
N(2)-C(3)-N(1)	110.8 (9)	N(4)-C(7)-N(3)	110.8 (9)
N(1)-C(1)-C(4)	122.3 (9)	N(3)-C(9)-C(12)	120.7 (9)
C(2)-C(1)-C(4)	128.7 (9)	C(8)-C(9)-C(12)	128.7 (10)
C(1)-C(2)-C(5)	133.0 (11)	C(9)-C(8)-C(11)	132.4 (12)
N(2)-C(2)-C(5)	120.0 (9)	N(4)-C(8)-C(11)	121.4 (10)
C(2)-N(2)-C(6)	128.8 (9)	C(8)-N(4)-C(10)	126.9 (9)
C(3)-N(2)-C(6)	124.3 (10)	C(7)-N(4)-C(10)	126.2 (10)
Perchlorate			
O(1)-Cl-O(2)	105.4 (6)	O(2)-Cl-O(3)	113.2 (6)
O(1)-Cl-O(3)	108.3 (6)	O(2)-Cl-O(4)	112.5 (5)
O(1)-Cl-O(4)	104.6 (6)	O(3)-Cl-O(4)	112.1 (5)

Table III. Deviations from Least-Squares Planes (Å) and Dihedral Angles (deg) for 1

plane I <sup>a</sup>		plane II <sup>a</sup>	
N(1)	-0.005	N(3)	-0.012
C(1)	-0.012	C(9)	-0.001
C(2)	0.013	C(8)	0.012
N(2)	0.016	N(4)	0.022
C(3)	-0.004	C(7)	-0.008
C(4)	-0.010	C(10)	-0.004
C(5)	0.007	C(11)	-0.015
C(6)	-0.005	C(12)	0.006
Dihedral Angles <sup>b</sup>			
CuN <sub>4</sub> /plane I	75.7	CuN <sub>4</sub> /plane II	75.5

<sup>a</sup> All atoms listed were used to define the plane. <sup>b</sup> The CuN<sub>4</sub> unit is strictly coplanar.

membered imidazole rings span the ranges 1.326 (12)–1.384 (11) Å and 105.5 (8)–110.8 (9)°, respectively, and compare well with those reported for similar structures.<sup>22,33</sup>

Both imidazole units nearly are coplanar (Table III) and are oriented approximately perpendicular to the CuN<sub>4</sub> unit; the dihedral angles between the best planes are 75.5 and 75.7°. This structural feature is similar to that reported for the tetragonal CuN<sub>4</sub>O<sub>2</sub> unit present in Cu(im)<sub>4</sub>·2NO<sub>3</sub>; the dihedral angles between the imidazole planes and the equatorial CuN<sub>4</sub> unit are 81.4 and 85.4°. In the related tetragonal CuN<sub>4</sub>O<sub>2</sub> complex Cu(im)<sub>4</sub>·SO<sub>4</sub>, these dihedral angles are 81.0 and 29.7° while in the tetragonal CuN<sub>4</sub>O<sub>2</sub> complex Cu(im)<sub>4</sub>·2ClO<sub>4</sub>, they are 85.7 and 18.7°. Possible electronic spectral consequences of these results are discussed below.

Inspection of Figure 1 offers a possible reason why the ClO<sub>4</sub><sup>-</sup> groups are nonligating in the title complex. Although the ClO<sub>4</sub><sup>-</sup> groups geometrically are oriented for potential apical Cu–OClO<sub>3</sub> bonding, actual bonding sterically is prohibited by the imidazole methyl groups C(4), C(12), etc. The tetragonal CuN<sub>4</sub>O<sub>2</sub> species noted above exhibit apical Cu–O bond distances of approximately

2.6 Å. Since the shortest Cu–O contacts in 1 are greater than 4 Å, apical bonding is considered to be absent. The perchlorate groups are held in lattice holes by Coulombic forces and exhibit no indications of disorder. The perchlorate bond distances (range 1.408 (8)–1.473 (8) Å) and angles (range 104.6 (6)–113.2 (6)°) agree with those reported for similar structures.<sup>34</sup>

**Electronic Structural Aspects of Alkylated Imidazoles.** In order to obtain better resolved  $\pi$ (imidazole)  $\rightarrow$  Cu(II) LMCT absorptions of solvated tetrakis(imidazole)copper(II) species, we found it necessary to use fairly bulky alkylated imidazole ligands. Consequently the electronic spectroscopic aspects associated with the alkylation of the imidazole ring are of some interest. The effects of ring methylation on the electronic structures of the free ligands have been explored by using INDO/S calculations, the results of which are summarized in Table IV. The spectroscopically relevant ligand orbitals are the three upper occupied molecular orbitals ( $\pi_1, \pi_2, n$ ) and the two vacant  $\pi^*$  orbitals; the lower lying occupied molecular orbitals are well removed in energy (>3 eV) from the  $\pi_2$  level. The INDO/S MO coefficients of the substituted imidazoles are very similar to those reported by Del Bene and Jaffé<sup>35</sup> for imidazole itself. The  $\pi_1$ (HOMO) orbital primarily has carbon 2p( $\pi$ ) character, whereas  $\pi_2$  is composed mainly of nitrogen 2p( $\pi$ ) orbitals; the n orbital essentially consists of the lone pair on the nitrogen donor atom. The calculated occupied orbital energies are in good agreement with the vertical ionization energies obtained from photoelectron spectra. For example, two separate studies of imidazole yielded similar vertical ionization energies for the  $\pi_1$  orbital (8.96<sup>36</sup> and 8.78 eV<sup>37</sup>), and both indicated that combined ionization from the  $\pi_2$  and n orbitals gave rise to a broad, unresolved absorption with a maximum at 10.3 eV. The calculated energies of the  $\pi_1, n$ , and  $\pi_2$  orbitals (Table IV) are -8.71, -10.16, and -10.61 eV, respectively. Ring methylation serves to lower the ionization energies. The observed vertical ionization energies for 1,2-dimethylimidazole are 8.38 eV ( $\pi_1$ ) and 9.79 eV ( $\pi_2, n$ )<sup>36</sup> and compare well with the values of -8.34, -9.88, and -10.09 eV calculated for the  $\pi_1, n$ , and  $\pi_2$  orbitals, respectively. Qualitatively, the electron-donating aspect of ring methyl groups is expected to destabilize these occupied  $\pi$  orbitals. More specifically, methylation of the ring carbon atoms (positions 2, 4, 5) ought to destabilize  $\pi_1$  (primarily carbon 2p( $\pi$ ) character) more than  $\pi_2$  (primarily nitrogen 2p( $\pi$ ) character), whereas methylation at nitrogen ought to destabilize  $\pi_2$  more than  $\pi_1$ . The calculated shifts in orbital energies quantify this expectation for the free ligands. Ring alkylation also serves to destabilize the ligand  $\pi^*$  orbitals slightly. It should be noted that histidine imidazole donors at protein sites are alkylated on either carbon 4 or 5.<sup>18</sup>

The spectroscopic consequences of ring alkylation are as follows. First, since the  $\pi_1, \pi_2, \pi^*$  orbital separation is decreased by ring alkylation at positions 2, 4, and 5, the first prominent UV absorption ( $\pi \rightarrow \pi^*$ ) is expected to red-shift. We have characterized the  $\pi \rightarrow \pi^*$  absorptions in methanol solution of imidazole (48 500 cm<sup>-1</sup>,  $\epsilon$  6900), 4,5-diethylimidazole (45 500 cm<sup>-1</sup>,  $\epsilon$  8000), 4,5-diisopropylimidazole (45 600 cm<sup>-1</sup>,  $\epsilon$  6000),<sup>14</sup> 1,2-dimethylimidazole (48 100 cm<sup>-1</sup>,  $\epsilon$  4300), and 1,4,5-trimethylimidazole (44 800 cm<sup>-1</sup>,  $\epsilon$  4570).<sup>38</sup> Thus, the calculated (Table IV) and observed red-shifts associated with the above patterns of di- and trialkylation amount to about 3500 cm<sup>-1</sup> (0.4 eV), except for 1,2-dimethylimidazole, which exhibits a considerably smaller (calculated and observed) red-shift. Although the calculated differences in excited-state energies agree with the experimentally determined values, the calculated values are too low by approximately 0.5 eV. For example, the  $\pi \rightarrow \pi^*$  absorption of imidazole

(34) Prochaska, H. J.; Schwindinger, W. F.; Schwartz, M.; Burk, M. J.; Bernarducci, E.; Lalancette, R. A.; Potenza, J. A.; Schugar, H. J. *J. Am. Chem. Soc.* **1981**, *103*, 3446–55. Ou, C. C.; Miskowski, V. M.; Lalancette, R. A.; Potenza, J. A.; Schugar, H. J. *Inorg. Chem.* **1976**, *15*, 3157–61.

(35) Del Bene, J.; Jaffé, H. H. *J. Chem. Phys.* **1968**, *48*, 4050–55.

(36) Ramsey, B. G. *J. Org. Chem.* **1979**, *44*, 2093–97.

(37) Craddock, S.; Findlay, R. H.; Palmer, M. H. *Tetrahedron* **1973**, *29*, 2173–81.

(38) This work.

Table IV. Effect of Ring Methylation on the Orbital and Excited-State Energies of Imidazole

orbital energies, eV	imidazole substituents					
	none	4-Me	4,5-Me <sub>2</sub>	1,2-Me <sub>2</sub>	1,4,5-Me <sub>3</sub>	1,2,4-Me <sub>3</sub>
$\pi^*$	1.30	1.39	1.45	1.49	1.53	1.57
$\pi^*$	0.18	0.24	0.33	0.43	0.43	0.44
$\pi_1$	-8.71	-8.46	-8.08	-8.34	-8.00	-8.08
$n$	-10.17	-10.06	-9.90	-9.88	-9.77	-9.84
$\pi_2$	-10.61	-10.40	-10.34	-10.09	-9.95	-10.01
	Excited States (eV)					
$n, \pi^*(f)^a$	4.37 (0.013)	4.37 (0.013)	4.34 (0.012)	4.46 (0.012)	4.34 (0.011)	4.46 (0.012)
$\pi, \pi^*(f)$	5.48 (0.184)	5.27 (0.171)	5.07 (0.203)	5.38 (0.204)	5.07 (0.195)	5.14 (0.193)
$n, \pi^*(f)$	5.82 (0.003)	5.82 (0.005)	5.76 (0.003)	5.76 (0.003)	5.74 (0.003)	5.79 (0.004)
$\pi, \pi^*(f)$	6.23 (0.091)	6.20 (0.094)	6.00 (0.110)	6.03 (0.070)	5.94 (0.085)	6.01 (0.077)

<sup>a</sup> Oscillator strength.

was observed at 48 500 cm<sup>-1</sup> (6.02 eV); the calculated value is 5.48 eV. The expected  $n \rightarrow \pi^*$  absorption calculated to occur at 4.37 eV apparently is too weak to be detected experimentally. A weak ( $\epsilon \sim 60$ ) absorption at 40 000 cm<sup>-1</sup> (4.96 eV) reported by earlier workers could not be reproduced in a more recent study.<sup>39</sup>

Second, since ring alkylation raises the energies of the  $\pi_1$ ,  $\pi_2$ , and  $n$  orbitals, Cu(II) complexes of alkylated imidazoles ought to exhibit red-shifted LMCT absorptions. The  $n$  orbital is destabilized by N-alkylation less than the  $\pi_1, \pi_2$  orbitals are destabilized by alkylation of the ring carbon atoms. The small red-shifts in  $n(\text{imidazole}) \rightarrow \text{Cu(II)}$  LMCT absorption expected from the calculated increase in  $n$  orbital energies (0.26–0.39 eV) are difficult to detect experimentally due to the overlapping and about equally red-shifted (0.10–0.41 eV) imidazole  $\pi \rightarrow \pi^*$  absorptions. Since the calculated difference in  $\pi_1, \pi_2$  orbital energies varies from 1.75 to 2.26 eV, some small energy differences between the  $\pi_1(\text{imidazole}) \rightarrow \text{Cu(II)}$  and  $\pi_2(\text{imidazole}) \rightarrow \text{Cu(II)}$  LMCT absorptions may be anticipated.

Third, ring alkylation is expected to affect the intensities of the  $\pi_1, \pi_2(\text{imidazole}) \rightarrow \text{Cu(II)}$  LMCT bands. This is because the alkyl substituents can affect the orientations between the imidazole rings and the Cu(II) d vacancy, particularly for solution complexes. Group theoretical considerations indicate that for tetragonal complexes ( $d_{x^2-y^2}$  ground state), these  $\pi(\text{imidazole}) \rightarrow \text{Cu(II)}$  LMCT absorptions should be polarized in the  $\text{CuN}_4$  plane ( $x, y$ ) for an imidazole ring oriented perpendicular to the  $\text{CuN}_4$  unit and polarized normal to the  $\text{CuN}_4$  plane ( $z$ ) for an imidazole ring coplanar with the  $\text{CuN}_4$  unit. However, intensity stealing from the strongly allowed in-plane ( $x, y$ )  $n(\text{imidazole}) \rightarrow \text{Cu(II)}$  LMCT absorptions should enhance only the in-plane  $\pi(\text{imidazole}) \rightarrow \text{Cu(II)}$  LMCT absorptions. The steric effects of imidazole alkylation should serve to orient the rings normal to the  $\text{CuN}_4$  units and thus result in fairly prominent LMCT absorptions. Ring orientation also may affect the energies of the  $\pi(\text{imidazole}) \rightarrow \text{Cu(II)}$  LMCT absorptions. Data pertinent to this issue currently are not available.

**Spectroscopic Studies of 1.** The electronic spectra of **1** and the free 1,4,5-trimethylimidazole ligand are shown in Figure 2 and summarized in Table V; ESR spectra of methanolic **1** are shown in Figure 3. The ESR spectra suggest that a mixture of tetragonal and rhombically distorted tetragonal species is present in methanolic solutions of **1** at 298 K.<sup>40</sup> However, characteristic tetragonal ESR spectra result when these solutions are cooled to approximately 220 K. This result is not particularly surprising. In the absence of excess ligand, the presence of some tris complex  $[\text{Cu}(1,4,5\text{-tmi})_3\text{CH}_3\text{OH}]$  is expected; such a species should exhibit rhombically distorted ESR spectra. It is important to note that the electronic spectra of methanolic **1** are unchanged over the temperature range 223–298 K. Apparently, the presence of some

Table V. Summary of Spectral Results and Assignments

system	solution <sup>a</sup>		mull <sup>b</sup> $\bar{\nu}$ , cm <sup>-1</sup>	assgnt
	$\bar{\nu}$ , cm <sup>-1</sup>	$\epsilon$		
1,4,5-trimethylimidazole	44 800	4570		$\pi \rightarrow \pi^*$
<b>1</b>	44 600	25100	~46 100	$\pi \rightarrow \pi^* +$ $n \rightarrow \text{Cu(II)}$
Cu(1,4,5-tmi) <sub>4</sub> ·2ClO <sub>4</sub>	32 800	2060	~34 500	$\pi_2 \rightarrow \text{Cu(II)}$
	28 700	1880	~26 200	$\pi_1 \rightarrow \text{Cu(II)}$
	16 800	50	~20 000	LF
Cu(im) <sub>4</sub> ·2NO <sub>3</sub>			~16 900	LF
			~40 000	$\pi_2 \rightarrow \text{Cu(II)}$
			~34 000	$\pi_1 \rightarrow \text{Cu(II)}$
1,2-dimethylimidazole			~19 000	LF
	48 100	4300		$\pi \rightarrow \pi^*$
	35 100 <sup>c</sup>	440	~32 800	$\pi_1 \rightarrow \text{Ni(II)}$
Ni(1,2-dmi) <sub>4</sub> ·2ClO <sub>4</sub>	22 200 <sup>c</sup>	130	~23 500	LF
	32 500	1860	~37 000	$\pi_2 \rightarrow \text{Cu(II)}$
	28 900	1920	~30 300	$\pi_1 \rightarrow \text{Cu(II)}$
Cu(1,2-dm) <sub>4</sub> ·2ClO <sub>4</sub>	16 800	50	~19 000	LF

<sup>a</sup> Measured at 298 K; concentration of the Cu(II) complexes was 0.035 M; concentration of Ni(II) in the neat Ni(II) complex is 2.26 M. <sup>b</sup> Mull spectra at 80 K. <sup>c</sup> Single-crystal spectra at 80 K.

not fully tetragonal Cu(II) species does not appreciably change either the LF or LMCT absorptions. Replacement of one nitrogen donor ligand by an oxygen-donor solvent molecule should result in minor displacements of the already broad LF and LMCT absorptions. However, the ESR spectra readily detect a reduction in chromophore symmetry of this type.

The solution electronic spectra of methanolic **1** essentially are identical with those exhibited by methanolic Cu(4,5-dialkylimidazole)<sub>4</sub><sup>2+</sup> chromophores.<sup>14</sup> The prominent ( $\epsilon$  25 100) UV absorption at 44 600 cm<sup>-1</sup> is assigned to the expected ligand  $\pi \rightarrow \pi^*$  absorption (44 800 cm<sup>-1</sup>,  $\epsilon \sim 4 \times 4570 = 18 300$ ) and overlapping  $n(\text{ligand}) \rightarrow \text{Cu(II)}$  LMCT absorption. The expected  $\pi_2(\text{ligand}) \rightarrow \text{Cu(II)}$  and  $\pi_1(\text{ligand}) \rightarrow \text{Cu(II)}$  LMCT absorptions are assigned to the well-resolved bands at 32 800 ( $\epsilon$  2060) and 28 700 cm<sup>-1</sup> ( $\epsilon$  1880), respectively. The expected LF absorption consists of the band at 16 800 cm<sup>-1</sup> ( $\epsilon$  50). The corresponding absorptions exhibited by polycrystalline **1** (mull spectra, 80 K) differ from the solution spectra in several ways. First, an additional LF absorption at ~20 000 cm<sup>-1</sup> is observed in the solid-state spectra. This result, along with the facts that polycrystalline **1** is orange-brown and methanolic solutions of **1** are blue-green, indicate that the solid-state and solution coordination geometries are somewhat different. Recent studies of various Cu(II)-ethylenediamine complexes indicate that rather subtle changes in coordination geometry such as perturbed apical ligation may cause substantial color changes associated with perturbed LF absorptions.<sup>41</sup> The absence of apical ligation observed for crystalline **1** may not be maintained in methanol solution. Some geometrical differences between crystalline and methanolic **1** also

(39) Grebow, P. E.; Hooker, T. M., Jr. *Biopolymers* **1975**, *14*, 871–81.(40) The LF and well-resolved LMCT spectra of approximately trigonal-bipyramidal Cu(alkylated imidazole)<sub>4</sub>solvent<sup>2+</sup> species will be reported elsewhere. Bernarducci, E.; Bharadwaj, P. K.; Soler, J.; Schugar, H. J., to be submitted for publication.(41) Grenthe, I.; Paoletti, P.; Sandström, M.; Glikberg, S. *Inorg. Chem.* **1979**, *18*, 2687–92.

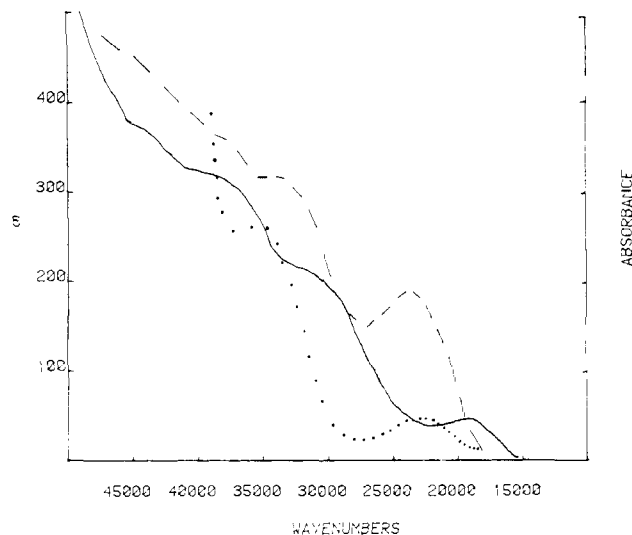


**Figure 4.** Comparison between the electronic spectra at 80 K of  $\text{Cu}(1,2\text{-dmi})_4 \cdot 2\text{ClO}_4$  (mull, —) and  $\text{Ni}(1,2\text{-dmi})_4 \cdot 2\text{ClO}_4$  (mull, ---; single crystal, ...).

are implied by shifts of 1500–2500  $\text{cm}^{-1}$  in the various UV absorptions. Moreover, the observed separation between the  $\pi_1, \pi_2(\text{ligand}) \rightarrow \text{Cu}(\text{II})$  LMCT absorptions is larger in the solid-state spectra ( $\sim 8300 \text{ cm}^{-1}$ ) than in the solution spectra ( $\sim 4100 \text{ cm}^{-1}$ ); the  $\text{Cu}(1,2\text{-dmi})_4 \cdot 2\text{ClO}_4$  complex exhibits similar behavior (see below). We do not yet understand the reasons for this latter effect.

As predicted, the higher energies of the  $\pi_1, \pi_2$  imidazole orbitals caused by ligand methylation have resulted in red-shifted LMCT absorptions. The structurally similar (see above) reference complex  $\text{Cu}(\text{im})_4 \cdot 2\text{NO}_3$  exhibits  $\pi(\text{imidazole}) \rightarrow \text{Cu}(\text{II})$  LMCT absorptions at  $\sim 40000$  and  $\sim 34000 \text{ cm}^{-1}$ ; corresponding absorptions in polycrystalline **1** have been red-shifted  $\sim 5500$  and  $\sim 8000 \text{ cm}^{-1}$ , respectively. The  $\pi_1(\text{imidazole}) \rightarrow \text{Cu}(\text{II})$  LMCT absorption of  $\text{Cu}(\text{im})_4 \cdot 2\text{NO}_3$  at  $\sim 34000 \text{ cm}^{-1}$  presumably corresponds to the shoulder at  $\sim 34000 \text{ cm}^{-1}$  ( $\epsilon \sim 3000$ ) that is present in the solution spectra of  $\text{Cu}(\text{im})_4^{2+}$ . Other workers have probed the orientation of the ligand rings in solvated  $\text{Cu}(\text{im})_4^{2+}$  by EPR<sup>42,43</sup> and spin-echo ESR studies.<sup>44</sup> Agreement on whether or not the imidazole rings exhibit a narrow spread of conformations has not been unanimous.<sup>42</sup> Owing to the weakness of the absorption at  $\sim 34000 \text{ cm}^{-1}$ , we suggest the imidazole rings of solvated  $\text{Cu}(\text{im})_4^{2+}$  do not have the large dihedral angles observed for all or some of the imidazole rings in crystalline  $\text{Cu}(\text{im})_4 \cdot \text{X}$  complexes ( $\text{X} = \text{SO}_4, 2\text{NO}_3, 2\text{ClO}_4$ ).<sup>22,33</sup> In contrast, methanolic **1** exhibits relatively intense ( $\epsilon \sim 2000$ )  $\pi(\text{ligand}) \rightarrow \text{Cu}(\text{II})$  LMCT absorptions presumably owing to preservation of the large ( $\sim 75^\circ$ ) dihedral angles present in crystalline **1**. As noted above, the perpendicular orientation of imidazole rings relative to the  $\text{CuN}_4$  unit/d vacancy ought to maximize the intensity of the  $\pi(\text{imidazole}) \rightarrow \text{Cu}(\text{II})$  LMCT bands. It is clear that answers to some of the above spectroscopic questions and a full account of imidazole  $\rightarrow$   $\text{Cu}(\text{II})$  LMCT absorptions requires polarized single-crystal studies of a series of variously structured chromophores; such studies are in progress.<sup>45</sup>

**M(1,2-dmi) $_4$ ·2ClO $_4$**  ( $\text{M} = \text{Ni}, \text{Cu}$ ). The assignment of imidazole/ $\text{Cu}(\text{II})$  charge-transfer absorptions as “metal-to-ligand” or “ligand-to-metal” depends upon whether the absorptions shift to higher or lower energies when  $\text{Cu}(\text{II})$  is replaced by less oxidizing divalent ions such as  $\text{Ni}(\text{II})$ . To facilitate this assignment, we have prepared and characterized in preliminary ways the yellow

diamagnetic complex  $\text{Ni}(1,2\text{-dmi})_4 \cdot 2\text{ClO}_4$  and a spectroscopic reference complex of the same ligand,  $\text{Cu}(1,2\text{-dmi})_4 \cdot 2\text{ClO}_4$ . Solid-state (mull and single crystal) spectra of the  $\text{Ni}(\text{II})$  complex are presented in Figure 4 and are summarized in Table V. Electronic spectra of the yellow-green methanolic solution complex probably are complicated by an equilibrium<sup>46</sup> between diamagnetic ( $S = 0$ )  $\text{NiN}_4^{2+}$  and paramagnetic ( $S = 1$ )  $\text{NiN}_4(\text{solvent})_2^{2+}$  chromophores and are not presented here. Solution and mull spectra of  $\text{Cu}(1,2\text{-dmi})_4 \cdot 2\text{ClO}_4$  are summarized in Table V; only the mull spectra are shown in Figure 4. Single crystals of the  $\text{Ni}(\text{II})$  complex exhibit an absorption at  $22200 \text{ cm}^{-1}$  ( $\epsilon 130$ ), which is a characteristic ligand field absorption of diamagnetic planar  $\text{NiN}_4^{2+}$  chromophores.<sup>47</sup> A higher energy absorption at  $35100 \text{ cm}^{-1}$  ( $\epsilon 440$ ) is assigned as  $\pi_1(\text{imidazole}) \rightarrow \text{Ni}(\text{II})$  LMCT (see below). As noted elsewhere,<sup>14</sup> the electronic structure, ligand  $\pi \rightarrow \pi^*$  absorptions, and ligand  $\rightarrow \text{Cu}(\text{II})$  LMCT absorptions of imidazole and pyrazole systems nearly are identical. Several diamagnetic  $\text{Ni}(\text{pyr})_4^{2+}$  chromophores<sup>48,49</sup> ( $\text{pyr} = \text{pyrazole}$ ) having planar  $\text{NiN}_4^{2+}$  units exhibit LF absorptions at  $\sim 23000 \text{ cm}^{-1}$  ( $\epsilon \sim 70$ ) along with absorptions at  $\sim 37000 \text{ cm}^{-1}$  ( $\epsilon \sim 1500$ ). These latter absorptions may be assigned as  $\pi_1(\text{pyrazole}) \rightarrow \text{Ni}(\text{II})$  LMCT. Corresponding absorptions of the structurally similar  $\text{Cu}(\text{pyr})_4^{2+}$  chromophores having planar  $\text{CuN}_4^{2+}$  units are red-shifted by  $\sim 6000 \text{ cm}^{-1}$ .<sup>48,49</sup>

We next consider the spectroscopic reference complex  $\text{Cu}(1,2\text{-dmi})_4 \cdot 2\text{ClO}_4$ . It is not yet known whether this complex contains a planar  $\text{CuN}_4$  or tetragonal  $\text{CuN}_4\text{O}_2$  coordination geometry. The  $\text{Ni}(\text{II})$  complex and this reference  $\text{Cu}(\text{II})$  complex exhibit different X-ray powder diffraction patterns. The methanolic solution spectra of  $\text{Cu}(1,2\text{-dmi})_4^{2+}$  are quite similar to those exhibited by  $\text{Cu}(1,4,5\text{-tmi})_4^{2+}$  and have been assigned in the same fashion (see Table V). Moreover, the separation between the  $\pi_1, \pi_2(\text{ligand}) \rightarrow \text{Cu}(\text{II})$  LMCT absorptions of  $\text{Cu}(1,2\text{-dmi})_4 \cdot 2\text{ClO}_4$  are greater in the solid-state spectra ( $\sim 6700 \text{ cm}^{-1}$ ) than in the solution spectra ( $\sim 3600 \text{ cm}^{-1}$ ). The lowest energy charge-transfer absorption of  $\text{Ni}(1,2\text{-dmi})_4 \cdot 2\text{ClO}_4$  is blue-shifted  $\sim 2500$ – $6600 \text{ cm}^{-1}$  relative to those exhibited by  $\text{Cu}(1,2\text{-dmi})_4 \cdot 2\text{ClO}_4$  and the title complex (**1**). The magnitude of this blue-shift is similar to that noted above for structurally similar  $\text{Ni}(\text{pyr})_4^{2+}$  and  $\text{Cu}(\text{pyr})_4^{2+}$  chromophores.

The assignment of these charge-transfer absorptions to LMCT rather than to MLCT is based upon the electronic natures of the ligands and the observed metal ion dependency of the band energies. In the classic treatment of charge-transfer absorptions of planar  $d^8$  metal complexes, those exhibited by the  $d^8$  tetrahalo complexes were assigned as LMCT.<sup>50</sup> This assignment was in harmony with the observed red-shift of these transitions as the oxidizing power of the  $d^8$  metal ions increased. Moreover, the chloride ligands did not have relatively stable  $\pi$ -acceptor orbitals. In contrast, cyanide ions have more stable  $\pi$ -acceptor orbitals, and a relatively stable molecular orbital in planar tetracyano-metallate complexes arises from the interaction of four ligand  $\pi^*$  orbitals with the metal  $p_z$  orbital. Such complexes exhibited charge-transfer absorptions that blue-shifted with increased oxidizing power of the  $d^8$  metal ion and accordingly were assigned as MLCT. The authors who pioneered the study of metal-pyrazole complexes mistakenly have assigned the observed charge-transfer bands as MLCT.<sup>48</sup> It is clear that the charge-transfer bands of structurally similar pyrazole (and imidazole) complexes red-shift as the metal ions become more oxidizing. A blue-shift would be expected if these absorptions were of the type  $d(\text{metal}) \rightarrow \pi^*(\text{ligand})$ . Our studies of tetrahedral  $\text{Ni}(\text{II})$  and  $\text{Co}(\text{II})$  imidazole chromophores also exhibit charge-transfer absorptions that are in harmony with a LMCT (but not MLCT)

(42) Mulks, C. F.; Kirste, B.; van Willigen, H. *J. Am. Chem. Soc.* **1982**, *104*, 5906–11.

(43) Van Camp, H. L.; Sands, R. H.; Fee, J. A. *J. Chem. Phys.* **1981**, *75*, 2098–2107.

(44) Mims, W. B.; Peisach, J. *J. Chem. Phys.* **1978**, *69*, 4921–30.

(45) Unpublished results of P. K. Bharadwaj and H. J. Schugar, Rutgers University, and A. Gewirth and E. I. Solomon, Stanford University.

(46) Fabbrizzi, L.; Micheloni, M.; Paoletti, P. *Inorg. Chem.* **1980**, *19*, 535–38.

(47) Bryan, P. S.; Dabrowiak, J. C. *Inorg. Chem.* **1975**, *14*, 299–302.

(48) Jesson, J. P.; Trofimenko, S.; Eaton, D. R. *J. Am. Chem. Soc.* **1967**, *89*, 3148–58.

(49) Herring, F. G.; Patmore, D. J.; Storr, A. *J. Chem. Soc., Dalton Trans.* **1975**, 711–17.

(50) Gray, H. B.; Ballhausen, C. J. *J. Am. Chem. Soc.* **1963**, *85*, 260–65.

formalism.<sup>51</sup> A suggestion that Cu(II)  $\rightarrow$  imidazole( $\pi^*$ ) MLCT absorptions contribute to the near UV spectra of type 1 Cu(II) recently has been published.<sup>52</sup> We are unable to discern any obvious justification for this suggestion.

### Conclusions

The association of well-resolved  $\pi_1, \pi_2(\text{ligand}) \rightarrow \text{Cu(II)}$  LMCT spectra with structurally constrained Cu(alkylated imidazole)<sub>4</sub><sup>2+</sup> chromophores has been further documented by crystallographic and spectroscopic studies of **1**. Steric effects of the 1,4,5-trimethylimidazole ligand serve to orient the ligand rings nearly perpendicular to the planar CuN<sub>4</sub> unit. ESR studies of methanolic **1** show that this structural feature may be retained by the tetragonal solution complex. INDO/S molecular orbital calculations show that ring methylation of imidazole raises the  $n$ ,  $\pi_1$ , and  $\pi_2$  orbital energies of imidazole and slightly destabilizes the vacant  $\pi^*$  orbitals as well. Di- and trimethylation of imidazole experimentally is observed to cause (a) a red-shift of the imidazole  $\pi \rightarrow \pi^*$  absorption of 400–3500 cm<sup>-1</sup> and (b) a red-shift of the  $\pi_2, \pi_1(\text{ligand}) \rightarrow \text{Cu(II)}$  LMCT absorptions of  $\sim 5000$  cm<sup>-1</sup>. The

energy separation between the  $\pi_2, \pi_1(\text{imidazole}) \rightarrow \text{Cu(II)}$  LMCT absorptions in the solid state ( $\sim 8000$  cm<sup>-1</sup>) is greater than that exhibited by solution Cu(im)<sub>4</sub><sup>2+</sup> chromophores ( $\sim 4000$  cm<sup>-1</sup>). Various Ni(II) tetrakisimidazole and tetrakispyrazole chromophores exhibit a  $\pi_1(\text{ligand}) \rightarrow \text{M(II)}$  LMCT absorption that is blue-shifted ( $>2500$  cm<sup>-1</sup>) from the corresponding absorption exhibited by structurally similar Cu(II) analogues. This result confirms the assignment as LMCT, not MLCT, and is supported by studies of pseudotetrahedral Cu(II), Ni(II), and Co(II) chromophores, which will be presented elsewhere.

**Acknowledgment.** This work was supported by the National Institutes of Health (Grant AM-16412 to H.J.S.), the Rutgers Computing Center, and the Rutgers Research Council (K.K.-J.).

**Registry No.** **1**, 85337-05-9; Ni(1,2-dmi)<sub>4</sub>·2ClO<sub>4</sub>, 39734-28-6; Cu(1,2-dmi)<sub>4</sub>·2ClO<sub>4</sub>, 39734-29-7; Cu(im)<sub>4</sub>·2NO<sub>3</sub>, 33790-63-5; 1,4,5-tmi, 20185-22-2; im, 288-32-4; 1,2-dmi, 1739-84-0; 4-methylimidazole, 822-36-6; 4,5-dimethylimidazole, 2302-39-8; 1,2,4-trimethylimidazole, 1842-63-3.

**Supplementary Material Available:** Stereoscopic packing diagram and tables of calculated hydrogen atom positions, anisotropic thermal parameters, and observed and calculated structure factors for **1** (11 pages). Ordering information is given on any current masthead page.

(51) Bernarducci, E. E.; Bharadwaj, P. K.; Lalancette, R. A.; Potenza, J. A.; Schugar, H. J., to be submitted for publication.

(52) Downes, J. M.; Whelan, J.; Bosnich, B. *Inorg. Chem.* **1981**, *20*, 1081-86.

## Computational Design of Polylactone Macrocyclic Ionophores<sup>§</sup>

Shneior Lifson,\*<sup>†</sup> Clifford E. Felder,<sup>†</sup> and Abraham Shanzer\*<sup>‡</sup>

Contribution from the Departments of Chemical Physics and Organic Chemistry, Weizmann Institute of Science, 76100 Rehovot, Israel. Received September 27, 1982

**Abstract:** Empirical energy functions of bond lengths, bond angles, torsional angles, and interatomic Coulombic and Lennard-Jones interactions are applied to predict ionophoric properties of macrocyclic polylactones. Equilibrium conformations and energies of candidate molecules and their complexes with Li<sup>+</sup>, Na<sup>+</sup>, and K<sup>+</sup> are derived. The ability to form a cage surrounded by polar groups is considered a necessary condition for ionophoric behavior. The calculated dimensions of the cage and its structural and symmetry properties, as well as the binding energy of the ion/molecule complex, are used as criteria for the efficiency and specificity of the ionophore. Calculations on DL-cyclohexalactyl, an enniatin analogue, are used to test the method. They indicate good ionophoric properties and preference for Na<sup>+</sup>, in qualitative agreement with experiment. Cyclic tetralactones with structural "reflection-symmetry" (ref-lactones) (C<sup>1</sup>O'(CH<sub>2</sub>)<sub>m</sub>OC<sup>1</sup>O'(CH<sub>2</sub>)<sub>n</sub>)<sub>2</sub> are all found to lack the conformational symmetries required for ionophoric behavior. Cyclic tripropiolactones with a rotational symmetry (roto-triropiolactones) (C<sup>1</sup>H<sub>2</sub>C<sup>2</sup>H<sub>2</sub>C<sup>1</sup>O'O)<sub>3</sub> are predicted to complex well with the alkali ions. Their dimers are predicted to form octahedral cages of almost perfect structure and symmetry. Hydrophobic side chains attached at either C<sup>1</sup> or C<sup>2</sup> in either equatorial or axial positions are considered as factors for stabilization of the dimer and its cage parameters. They confer chirality on the molecule (L or D) and lead to two dimer/ion complexes (LL or LD). Isopropyl substituents are found not to be large enough to make hydrophobic contact in the LD configuration but do form stable cages in LL when attached to C<sup>2</sup>, with preference for Na<sup>+</sup>.

### Introduction

Ionophores, otherwise known as ion carriers or complexones, are naturally occurring cyclic molecules whose biological function is to transport ions across lipid membranes of living cells.<sup>1</sup> Since this function is essential for the very existence of a wide variety of life processes, a large number of ionophores of specific and highly optimized properties are found in nature. They bind ions very efficiently and subsequently release them with the same ease.<sup>2</sup> Some of them are amazingly selective for specific ions, and all of them reduce the electric resistance of lipid membranes by several orders of magnitude.

Although ionophores may vary widely in chemical composition and molecular size, they all function using the same principles. A comprehensive discussion of the thermodynamics and kinetics

(1) C. Moore and B. C. Pressman, *Biochem. Biophys. Res. Commun.*, **15**, 562 (1964); B. C. Pressman, E. J. Harris, W. S. Jagger, and J. H. Johnson, *Proc. Natl. Acad. Sci. U.S.A.*, **58**, 1949 (1967); Yu. A. Ovchinnikov, V. T. Ivanov, and A. M. Shkrob, *BBA Libr.*, **12** (1974); Yu. A. Ovchinnikov, in "Frontiers in Bioorganic Chemistry and Molecular Biology", Yu. A. Ovchinnikov and M. N. Koslov, Ed., Elsevier/North Holland Biomedical Press, Amsterdam, 1979, p 129; B. C. Pressman, *Ann. Rev. Biochem.*, **45**, 501 (1976).

(2) H. Diebler, M. Eigen, G. Ilgenfritz, G. Maass, and R. Winkler, *Pure Appl. Chem.*, **20**, 93 (1969); G. Eisenman and S. J. Krasne, "The Ion Selectivity of Carrier Molecules, Membranes and Enzymes", Chapter 2, and W. Epstein, "Membrane Transport", Chapter 10, in *MTP Int. Rev. Sci. Biochem. Ser.*, Vol. 2, Butterworths, London, 1975.

<sup>§</sup> Dedicated to Prof. Jack D. Dunitz on the occasion of his 60th birthday.

<sup>†</sup> Department of Chemical Physics.

<sup>‡</sup> Department of Organic Chemistry.